PCCP
Physical Chemistry Chemical Physics

Accepted Manuscript

This article can be cited before page numbers have been issued, to do this please use: A. Listkowski, R. Luboradzki, M. Gil, A. Gorski and J. Waluk, *Phys. Chem. Chem. Phys.*, 2026, DOI: 10.1039/D6CP01735E.

This is an Accepted Manuscript, which has been through the Royal Society of Chemistry peer review process and has been accepted for publication.

Accepted Manuscripts are published online shortly after acceptance, before technical editing, formatting and proof reading. Using this free service, authors can make their results available to the community, in citable form, before we publish the edited article. We will replace this Accepted Manuscript with the edited and formatted Advance Article as soon as it is available.

You can find more information about Accepted Manuscripts in the Information for Authors.

Please note that technical editing may introduce minor changes to the text and/or graphics, which may alter content. The journal's standard Terms & Conditions and the Ethical guidelines still apply. In no event shall the Royal Society of Chemistry be held responsible for any errors or omissions in this Accepted Manuscript or any consequences arising from the use of any information it contains.

ROYAL SOCIETY OF CHEMISTRY

rsc.li/pccp

View Article Online
DOI: 10.1039/D6CP01735E

A minor substituent modification leads to a large change in photophysics: 9,20-dialkyl-substituted porphycenes

Arkadiusz Listkowski,[1,2]* Roman Luboradzki,[1] Michał Gil,[1] Aleksander Gorski,[1] Jacek Waluk[1]*

[1]*Institute of Physical Chemistry, Polish Academy of Sciences, 01-224 Warsaw, Kasprzaka 44/52, Poland;* [2]*Faculty of Mathematics and Science, Cardinal Stefan Wyszynski University, Dewajtis 5, 01-815 Warsaw, Poland*

*Corresponding authors, email: a.listkowski@uksw.edu.pl, jwaluk@ichf.edu.pl

ABSTRACT

Porphycene – constitutional isomer of porphyrin - exhibits spectral and photophysical properties that surpass those of the parent macrocycle in the context of potential applications. Three novel derivatives of porphycene bearing two cyclohexyl, isopropyl or *tert*-butyl functionalities at the *meso* positions (9,20) have been obtained and characterized by structural and spectroscopic techniques combined with quantum chemical calculations. Substitution with isopropyl or cyclohexyl does not significantly affect fluorescence quantum yields and lifetimes with respect to parent, unsubstituted porphycene. In contrast, introducing two *tert*-butyl moieties at the *meso* positions results in extremely weak emission, which, however, can be recovered by placing the chromophore in a viscous environment. This is explained by large amplitude geometry relaxation in the lowest excited singlet state, leading to enhanced $S_0 \leftarrow S_1$ internal conversion. Since nonradiative S_1 deactivation occurs directly to S_0, the triplet state is not populated, and no singlet oxygen is produced. Porphycenes that exhibit such photophysical properties emerge as prospective functional materials in areas that exploit light matter-interactions. Factors that make these compounds so attractive include (a) strong absorption in the long wavelength range of visible spectrum; (b) extreme sensitivity of emission intensity to viscosity of the environment; (c) very good photostability, (d) non-toxicity, and (e) possibility of use as fluorophores in the single molecule regime.

INTRODUCTION

Porphycenes, constitutional isomers of porphyrins, are attractive candidates for application in photodynamic therapy of cancer (PDT),[1] photodynamic inactivation of bacteria (PDI),[2] as catalytic agents[3] or artificial metalloenzymes.[4] They are well known as good emitters,[5-7] due to the radiative constant of S_1 depopulation being much larger in porphycene[7] than in porphyrin.[8] Parent, unsubstituted porphycene emits fluorescence with the quantum yield of about 50%,[7] whereas the

View Article Online
DOI: 10.1039/D6CP01735E

emission of porphyrin is an order of magnitude lower.[9] However, not all porphycenes emit strongly. In particular, substitution at the *meso* positions can dramatically lower the fluorescence intensity. A good example is 9,10,19,20-tetramethylporphycene, of which the fluorescence quantum yield is about 10^{-4} in commonly used solvents.[10] Interestingly, fluorescence is strongly enhanced when the molecule is embedded in a rigid environment, such as a cryogenic matrix or low temperature glass or a viscous liquid or polymer film at room temperature. Viscosity dependent fluorescence has now been reported for several porphycenes.[7, 10-13] Particularly intriguing is that the emission intensity can be changed not only by the nature of the substituents, but also by the number of functionalities and their relative position. Removing two methyl groups from the tetra-alkyl-substituted porphycene mentioned above results in the recovery of fluorescence intensity.[7] Equally interesting is the comparison of photophysical properties of *meso*-dicyclopentyl- and *meso*-dicyclohexylporphycene.[11] The fluorescence quantum yield of the latter is more than two orders of magnitude lower than that of the former.

Our strategy to understand the mechanisms responsible for variations of spectral and photophysical characteristics in porphycenes is to investigate structurally similar derivatives while varying the number of substituents, their positions, electron donating/accepting characteristics, as well as their size. In this work, we investigate three novel compounds, derivatives of porphycene bearing alkyl substituents at the *meso* positions 9 and 20 (Scheme 1). The photophysical properties of cyclohexyl and isopropyl derivatives, **1** and **2**, respectively, are very similar to those of the parent porphycene. However, a spectacular effect is observed when 2-isopropyl substituents are replaced with *tert*-butyl ones, leading to **3**. Fluorescence of **3** strongly decreases with respect to **1** and **2**, but it can be recovered by changing the solvent to a viscous one, such as glycerol. Detailed analysis of

View Article Online
DOI: 10.1039/D6CP01735E

photophysical properties of **3** reveals characteristics that are attractive in the context of possible practical applications.

Scheme 1

RESULTS

Syntheses

In order to obtain the desired 9,20-disubstituted porphycenes, we followed a strategy based on the McMurry cross reaction, which we had successfully used before to obtain methyl and phenyl derivatives of this type.[7, 14] The reaction of an equimolar mixture of 2,2'-diformyl-5,5'-bipyrrole with the appropriate diketone (**2a-c**) should lead to the desired product, which, however, needs to be isolated from a mixture that may also contain unsubstituted porphycene and porphycene substituted in all four *meso* positions (Scheme 2). This isolation is generally troublesome and, in previous cases, required performing two careful chromatographic separations. Interestingly, in the case of the expected derivatives containing cyclohexyl, isopropyl, and *tert*-butyl groups in the *meso* positions, most of these problems were avoided. In all three cases, the only reaction products were the expected 9,10-disubstituted porphycene and the unsubstituted porphycene. Formation of tetrasubstituted products was not observed, likely due to crowding at the adjacent *meso* positions. Furthermore, the polarity difference between the new porphycenes and the unsubstituted one was sufficiently large, so that chromatographic separation of the mixture posed no problems. The obtained yields of the expected products were of the order of 1-2%, which is, unfortunately, typical for this type of reaction.

Scheme 2

Structure

View Article Online
DOI: 10.1039/D6CP01735E

NMR spectra. All the new compounds were characterized by mass spectrometry as well as NMR spectroscopy (see Table 1 and Supporting Information). The NMR spectra of compounds **1** and **2** in the aromatic region are very similar. Because of tautomerization interconverting two degenerate *trans* tautomers, two upper pyrrole rings become equivalent; the same happens for the two lower ones. The characteristic singlet coming from the hydrogen atom located at the *meso* position (H10/H19) appears at 9.70 in **1** and at 9.71 ppm in **2**. Doublets from H3/H6, H13/H16, H2/H7, and H12/H17 appear in **1** at 9.62, 9.53, 9.40 and 9.11 ppm and at 9.63, 9.55, 9.41 and 9.13 ppm in **2**. In the region corresponding to aliphatic protons, where the signals originating from substituents appear, the differences are, as expected, very pronounced. In **1**, the signal of the hydrogen atom bonded to the carbon atom of the cyclohexyl ring directly attached to the porphycene ring appears at around 4.90 ppm, whereas in the region from 2.80 to 1.60 ppm six multiplets can be observed. These correspond to the remaining protons of the cyclohexyl ring, taking into account the differences resulting from their positions in the chair conformation of the six-membered ring. For compound **2**, only two signals are present in this region. At 5.36 ppm, a signal originating from the CH group appears, while at 2.13 ppm a doublet from the CH_3 group is observed. A clearly visible NH signal can also be detected at a chemical shift of 4.67 ppm. The slight differences in the chemical shifts of the proton signals in the aromatic region for compounds **1** and **2** can be readily explained by the small structural difference between the cyclohexyl and isopropyl substituents within a distance of up to two carbon atoms from the porphycene ring. In the case of porphycene **3** with the *tert*-butyl group at the *meso* position, this difference is much greater, which is reflected in the spectrum of this compound. The singlet corresponding to the H10/H19 proton, located in the immediate vicinity of the substituent, is clearly shifted downfield (9.97 ppm) compared to compounds **1** and **2**. A similar situation is observed for the signal originating from

View Article Online
DOI: 10.1039/D6CP01735E

the H2/H7 proton, which appears as an AB system at 9.58 ppm and which interchanges its order in the spectrum with the H13/H16 proton compared to the two derivatives discussed above. The remaining protons, located farther from the *tert*-butyl group, resonate at magnetic field values similar to those observed for compounds **1** and **2**. The signal for the H3 proton appears at 9.63 ppm, H13 at 9.49 ppm, and H12 at 9.11 ppm. The positions of the NH protons, however, change significantly. They resonate at much lower field values (5.24 ppm), suggesting the presence of a considerably stronger hydrogen bond in porphycene **3** compared to porphycenes **1** and **2**. This is most likely related to the shortening of the distance between the Na and Nb atoms, caused by the presence of the bulky *tert*-butyl group at the crowded *meso* position. A direct attempt to prove this by measuring the relevant distances in the crystals was unsuccessful. In case of compounds **1** and **2** we were able to prepare crystals suitable for the X-ray analysis, however, for compound **3**, such attempts were unsuccessful. An argument for a stronger hydrogen bond in **3** was provided by calculations, which predict a significantly lower frequency of the NaH stretching vibration compared to **1** and **2** (Tables S1-S3).

Table 1

Tautomeric forms. Calculations predict similar relative energy patterns for all three molecules (Figures S1-S3). Rotation of the substituent about the C(*meso*)-C(substituent) bond is described by a double minimum potential, with the C(β)C(*meso*)C(substituent)H dihedral angle being either 0 or 180^{o}. The former situation is energetically more favorable. For doubly substituted porphycenes, this leads to three trans rotameric forms, separated from each other by about 2-3 kcal/mol. The middle energy species (trans2) is not degenerate, contrary to the other two forms, but it can be treated as such, since the energies of formally different two trans2 tautomers are practically the same.

View Article Online
DOI: 10.1039/D6CP01735E

Porphycenes can also exist in the *cis* tautomeric forms, which are not degenerate. The lower energy species corresponds to the structure with both NH protons located on the nitrogen atoms separated by two bonds from the position of substitution (upper N atoms in Scheme 1). Their calculated energies were nearly isoenergetic with those of second lowest *trans* tautomers of **1** and **2**, whereas for **3** the cis form was predicted to be significantly more stable, lying ca. 1.5 kcal/mol above the lowest energy trans form, whereas the corresponding value for the second trans tautomer was 2.8 kcal/mol.

Inspection of relative energies of the lowest five forms shows that for the cis species the ZPE-corrected energies are stabilized with respect to non-corrected values, decreasing the cis – trans separation (Figures S1-S3). This can be explained by significant differences in the frequencies of the NH stretching vibrations, which are predicted to be much lower in the cis forms (Tables S1-S3). In other words, the two intramolecular hydrogen bonds are stronger in the cis tautomers. One should note, however, that the lowest energy species in **1** - **3** (as well as in parent **Pc**) corresponds to the trans form. The two H-bonds are equivalent in the cis, but not in the trans species, as is clearly indicated by the calculated NH stretching frequencies, differing by nearly 100 cm^{-1}. Interestingly, the N-N distances are calculated to be the same for both H-bonds; what makes one of them stronger is the greater linearity: the NHN angle is smaller in the weaker bond. The same factor seems to be responsible for the energy splitting between the cis forms: again, N-N distances are the same in cis1 and cis2, but the NHN angle is larger in cis1.

We also note that, due to the nonequality of H-bonds, the NH stretching vibrations are localized in the trans species, In the cis forms, where the two bonds are equivalent, the NH stretching modes are delocalized, forming a symmetric and antisymmetric combinations of a single NH stretch; the lower frequency is always obtained for the latter.

View Article Online
DOI: 10.1039/D6CP01735E

The X-ray data obtained for **1** and **2** (Figure 1) are consistent with the lowest energy geometry calculated for **2**, while for **1** the cyclohexyl fragment is disordered into two positions corresponding to the lowest calculated energy geometry (with 75% occupancy) and to the second highest energy *trans* form (with 25% occupancy).

The attempts to obtain the X-ray structure of **3** were unsuccessful.

Figure 1

Spectroscopy and photophysics

Absorption and fluorescence spectra, shown in Figure 2 are typical for porphycenes. Absorption consists of two band series, Q bands located in the red part of the spectrum at around 650, 620 and 580 nm (in toluene) and the stronger Soret band located in the violet part at around 370 nm. A characteristic three finger-like pattern is observed in the Q region, indicating that the spectra originate from one species. This is in agreement with the theoretical predictions that one *trans* form has a lower energy than the other two. A possible exception is the spectrum of **1** in acetonitrile, where the shape of the lowest transition band suggests the presence of two forms. Fluorescence decay is monoexponential, but one can expect very similar fluorescence lifetimes for different rotamers.

Figure 2

Typical for porphycenes, both absorption and fluorescence show hypsochromic shifts in polar solvents. The shifts are rather minor, except for **3** in glycerol, of which the fluorescence is substantially blue-shifted with respect to the emission in acetonitrile. It is also much stronger in glycerol, suggesting that a large amplitude structural change occurs in **3** in nonviscous solvents after electronic excitation.

View Article Online
DOI: 10.1039/D6CP01735E

1 and **2** exhibit high fluorescence quantum yields, practically the same in nonpolar toluene and polar acetonitrile (Table 2). The ratio of fluorescence lifetimes in these two solvents is equal to the ratio of squared refractive indices $(n_1/n_2)^2$. Thus, the intrinsic rate constants of radiationless S_1 depopulation are the same for **1** and **2**. Division by n^2 yields for **1** the values of $2.5 \cdot 10^7$ and $2.3 \cdot 10^7 s^{-1}$ for toluene and acetonitrile, respectively. For **2**, the corresponding values are $2.4 \cdot 10^7$ and $2.3 \cdot 10^7$ s^{-1}. They are, within experimental error, the same as reported for parent porphycene: $2.3 \cdot 10^7$ s^{-1} in both solvents.[7] These results are not unexpected, since porphycene is a hard chromophore,[15] i.e., one for which the electronic transition moments of Q transitions should not be influenced by "mild" perturbation, such as alkyl substitution.

Molecule **3** reveals completely different photophysical behaviour. Its fluorescence quantum yield in both toluene and acetonitrile is 100 times weaker than in **1** and **2**. The lifetime decreases drastically compared with **1** and **2**, falling below 50 ps, so that it could not be reliably measured by our time-resolved single photon counting setup. However, it could be readily obtained for **3** dissolved in glycerol. A value of 2.0±0.1 ns was obtained, indicating that fluorescence in this viscous environment is many times stronger than in toluene or acetonitrile. It is, however, still several times weaker than the emission of **1** and **2**.

Table 2

The value of the short S_1 lifetime in **3** observed in non-viscous solvents was determined using femtosecond transient absorption (TA) spectroscopy (Figure 3). The bleaching and TA signals decay with the same lifetimes of 15 ps in acetonitrile and 21 ps in toluene. We note that the longer decay in toluene is in line with its higher viscosity relative to acetonitrile (0.56 vs 0.35 cP at 298 K, respectively).[16] Importantly, no TA signal is observed beyond that time delay, indicating that the radiationless deactivation occurs via $S_0 \leftarrow S_1$ internal conversion, without populating the triplet

View Article Online
DOI: 10.1039/D6CP01735E

state. This conclusion was corroborated by the measurements of singlet oxygen formation efficiency (*vide infra*).

In contrast to **3**, $T_1 \leftarrow S_1$ intersystem crossing is efficient in **1** and **2**. Pump-probe experiments carried out in the nanosecond range showed that the ground state repopulation occurs via two channels: (a) fast, corresponding to the S_1 lifetime and (b) slow, due to $S_0 \leftarrow T_1$. Using the values of amplitudes obtained by fitting the kinetic traces to a biexponential function (Figure 4), the quantum yield of triplet formation equal to 0.38±0.5 was obtained for the solution of **2** in toluene.

Figures 3-4

Singlet oxygen yield and triplet formation efficiency. The quantum yield of singlet oxygen formation (Φ_Δ) was determined by the method based on the comparison of intensities of $^1O_2$ phosphorescence generated by the porphycene and the reference compound, phenalenone (Figure 5). **1** and **2** revealed practically the same value of Φ_Δ, 0.22 (Table 2) whereas for **3** no singlet oxygen formation was detected. In view of the TA results showing that the triplet state is not populated in **3**, such result could be expected.

Figure 5

Photostability. Since the photophysical parameters of **1** and **2** strongly differ from those of **3**, one can expect that the latter should be more photostable, due to bypassing the long-lived and therefore more reactive triplet route. This was confirmed by experiments. Absorption spectra of **2** and **3** in toluene were monitored at regular time intervals while irradiating with a 360 nm LED. Irradiation led to slow decomposition of **2** (Figure 6). Using a previously developed protocol,[17] the photobleaching quantum yield of 2×10^{-8} was obtained. On the other hand, no change in absorption was detected even after prolonged irradiation of solution of **3**. Assuming that our spectrometer can

View Article Online
DOI: 10.1039/D6CP01735E

reliably detect changes in absorption that are larger than 0.01, we can estimate an upper limit of 10^{-9} for the photodegradation quantum yield of **3**, a value showing excellent photostability of this compound. In fact, even the value for the less photostable porphycene is much higher than those reported for porphyrins.[18, 19]

Figure 6

DISCUSSION

Comparison of structural, spectral, and photophysical properties of three novel porphycenes demonstrated that a seemingly minor structural modification can lead to huge changes in photophysics. Even though similar effects have been described before for porphycenes,[7, 11, 12] the structural differences between strongly and weakly emitting chromophores were larger than those reported in the present work. Thus, decrease of fluorescence intensity was observed when doubly *meso*-alkyl-substituted porphycenes were converted into fourfold-substituted ones[7] or when a cyclopentyl moiety at the *meso* position was replaced by cyclohexyl[11, 12]. In the present case, switching from emissive to a nearly non-emissive regime is caused by replacement of a single hydrogen atom on the isopropyl substituent by a methyl group.

We have previously noticed an inverse correlation that exists between the intramolecular hydrogen bond strength in porphycenes, expressed by the NH – N distance, and the fluorescence quantum yield. For *meso*-alkyl substituted derivatives a huge (3 orders of magnitude!) drop of emission intensity was observed when this distance decreased from ca. 256 to 252 pm.[13] Unfortunately, the X-ray data of **3** were not of sufficient quality to be compared with those obtained for **1** and **2**. Still, the calculations (Tables S1-S3) correctly predict a shorter distance in **3** compared to **1** and **2**.

View Article Online
DOI: 10.1039/D6CP01735E

The sensitivity of emission to viscosity is a strong indication that a large amplitude geometry distortion, such as loss of planarity, occurs upon electronic excitation.

SUMMARY AND CONCLUSIONS

Porphycenes that exhibit extreme sensitivity of fluorescence intensity to viscosity, as described here for **3**, are promising candidates for being used as viscosity probes. What makes them attractive compared with the sensors used so far – molecular rotors[20, 21] – is the insensitivity to solvent polarity. The dipole moments of alkyl and aryl derivatives of porphycenes are usually very low; moreover, they do not change upon electronic excitation.

Another factor that bodes well for practical application of this class of porphycenes is the high photostability. Due to fast and efficient $S_0 \leftarrow S_1$ internal conversion, the triplet state – a usual channel for photodegradation – is not populated. Therefore, no singlet oxygen is generated and the probability of photodestruction is very low (in fact, it is already low even for porphycenes that populate the triplet). It is also naturally very low in S_1 because of its short lifetime.

Yet another advantage of using porphycenes is provided by their strong absorption in the red region. Molar absorption coefficient is about 50 000 $M^{-1}cm^{-1}$, which is much higher than in commonly used porphyrins.

One could argue that a very low emission quantum yield in "normal", routinely used solvents is a disadvantage for such possible application as fluorescence imaging. However, when working in the single molecule regime, weakly emitting molecules that do not cross into the triplet state upon excitation may emit more photons per time unit than the good fluorophores, if the latter populate the triplet with considerable yield.[22] In addition, no singlet oxygen is generated because of lack of

View Article Online
DOI: 10.1039/D6CP01735E

triplet population; as a consequence, the fluorophore is expected to be non-toxic, which is crucial for biology and medicine-related applications.

Porphycenes emerge as an extremely promising class of functional materials. The main obstacle for widespread use is that their syntheses are quite challenging.[23, 24] Hopefully, the synthetic progress will lead in the future to their availability, enabling applications of these fascinating compounds in various areas.

SUPLEMENTARY MATERIAL

See Supporting Information for synthetic and experimental details, NMR spectra, and geometries of optimized molecular structures.

ACKNOWLEDGEMENTS

This research was funded by the Polish National Science Centre, grant 2019/35/B/ST4/00297. We gratefully acknowledge Poland's high-performance Infrastructure PLGrid AGH, for providing computer facilities and support within computational grant PLG/2025/019151.

DATA AVAILABILITY

The data that support the findings of this study are available from the corresponding author upon reasonable request.

View Article Online
DOI: 10.1039/D6CP01735E

Table 1. Proton NMR shifts. For more details, see Supporting Information.

1	2	3
9.70 H-10 and H-19 9.62 H-3 and H-6 9.53 H-13 and H-16 9.40 H-2 and H-7 9.11 H-12 and H-17 4.90 H-9^{1ax} and H-20^{1ax} 2.70-2.63 H-9^{2eq} and H-20^{2eq} 2.53-2.42 H-9^{2ax} and H-20^{2ax} 2.28-2.18 H-9^{3eq} and H-20^{3eq} 2.73-2.15 H-9^{4eq} and H-20^{4eq} 2.03-1.91 H-9^{3ax} and H-20^{3ax} 1.72 H-9^{4ax} and H-20^{4ax});	9.71 H-10 and H-19 9.63 H-3 and H6 9.55 H-13 and H-16 9.41 H-2 and H7 9.13 H-12 and H-17 5.36 2×-C$\underline{H}$(CH$_3$)$_2$) 4.67 NH 2.13 2×-CH(C$\underline{H}_3$)$_2$	9.91 H-10 and H-19 9.63 H-3 and H-6 9.58 H-2 and H-7 9.49 H-13 and H-16 9.11 H-12 and H-17) 5.24 NH 2.43 2×C(C$\underline{H}_3$)$_3$)

Table 2. Fluorescence quantum yields (φ_{fl}), lifetimes (τ_{fl}), and the quantum yield of singlet oxygen formation (Φ_Δ), measured at 293 K.

	φ_{fl}		τ_{fl} [ns][a]		Φ_Δ
	Toluene	Acetonitrile	Toluene	Acetonitrile	Acetonitrile
1	0.31 ± 0.03	0.29 ± 0.03	5.6 ± 0.1	7.2 ± 0.1	0.22 ± 0.02
2	0.31 ± 0.03	0.30 ± 0.03	5.8 ± 0.1	7.2 ± 0.1	0.22 ± 0.02
3	0.003 ± 0.001	0.003 ± 0.001	0.015 ± 0.002	0.021 ± 0.002	< 0.01

[a] Determined using time-resolved single photon counting for **1** and **2**, and from transient absorption measurements for **3**.

View Article Online
DOI: 10.1039/D6CP01735E

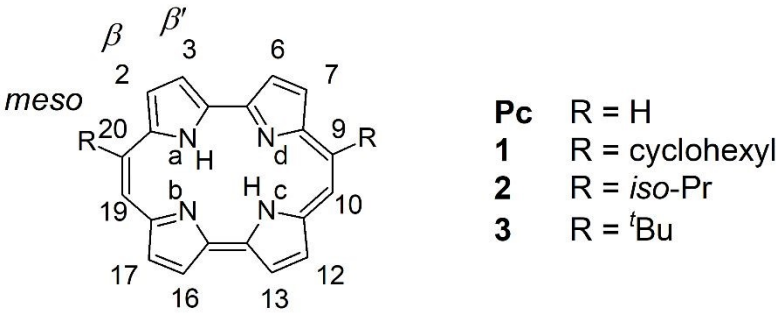

Pc R = H
1 R = cyclohexyl
2 R = *iso*-Pr
3 R = ^{t}Bu

Scheme 1. Parent (**Pc**) and the novel porphycenes.

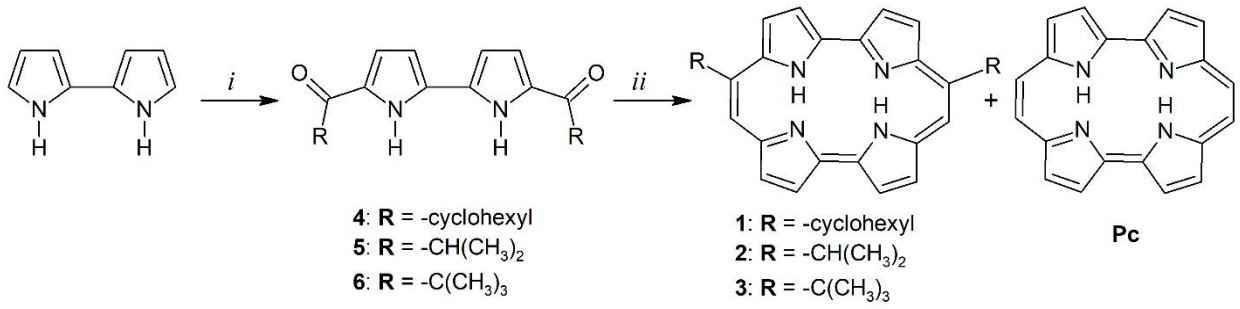

Scheme 2. Reagents and conditions: *i*. 1. $RCON(Et)_2$, $CHCl_3$, $POCl_3$, 65°C, overnight; 2. NaOAc, H_2O, 90°C, 2h; *ii*. 1. Zn/CuCl. THF, Δ, 2h; 2. 5,5'-diformyl-2,2'-bipyrrole, Δ.

View Article Online
DOI: 10.1039/D6CP01735E

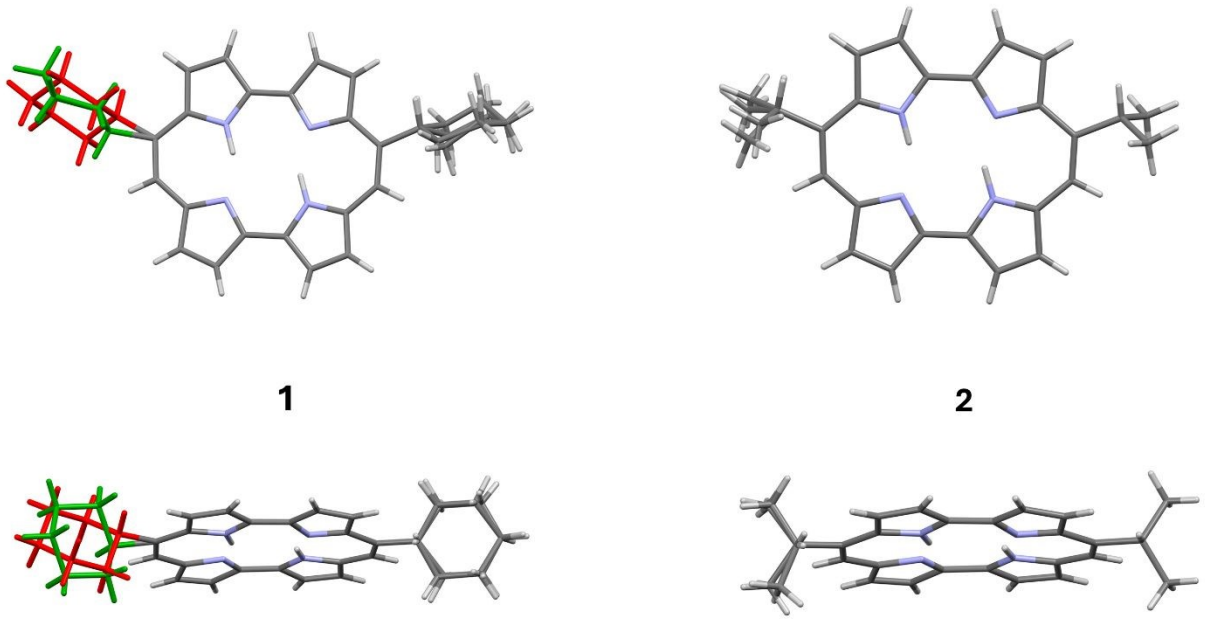

Figure 1. X-ray structures of **1** and **2**. The disordered positions of the cyclohexyl fragment indicated by colors: red (75% occupancy) and green (25% occupancy).

View Article Online
DOI: 10.1039/D6CP01735E

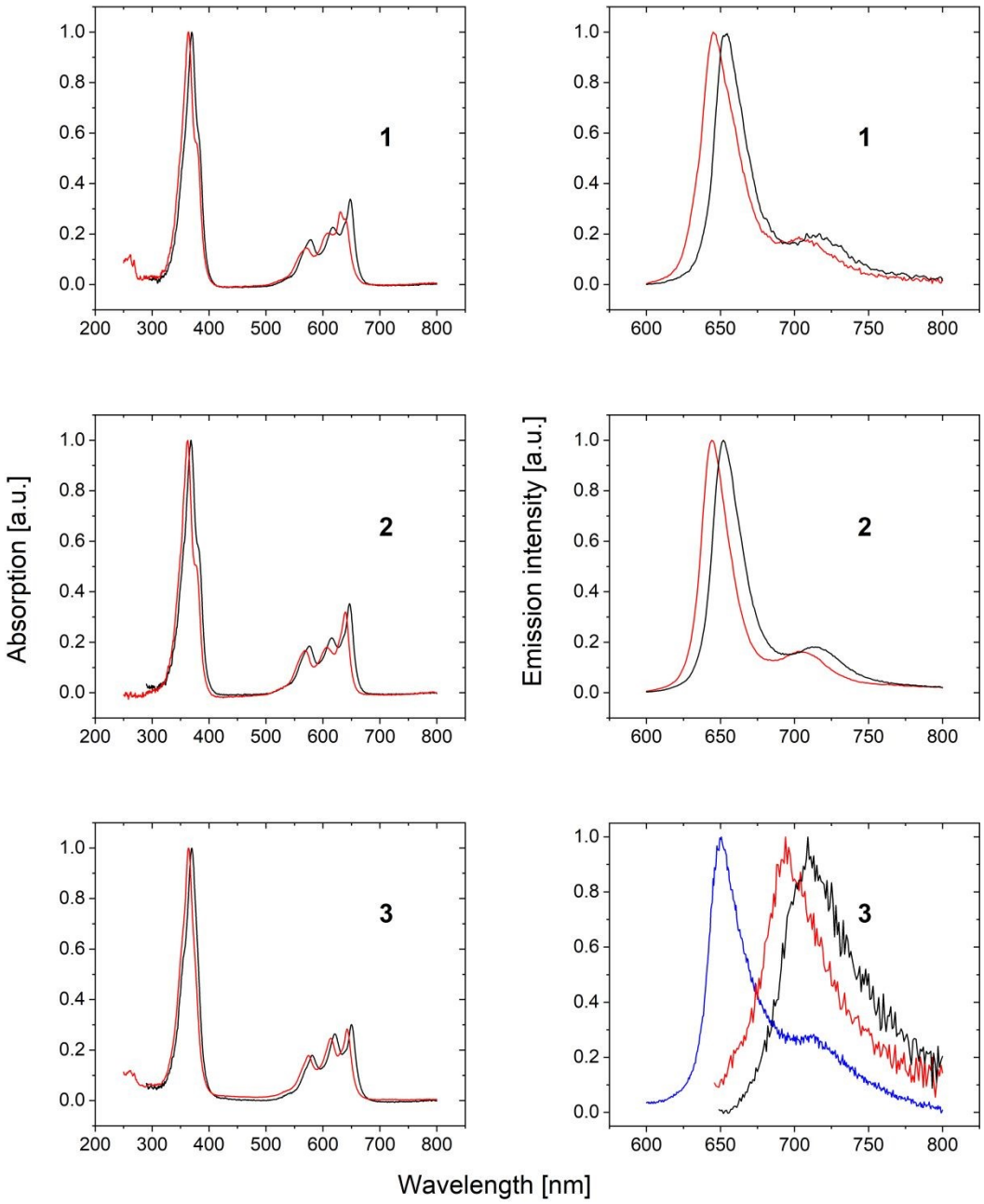

Figure 2. Left, normalized absorption, right, normalized fluorescence spectra at 293 K recorded for 10^{-5} M solutions in toluene (black), acetonitrile (red) and glycerol (blue).

View Article Online
DOI: 10.1039/D6CP01735E

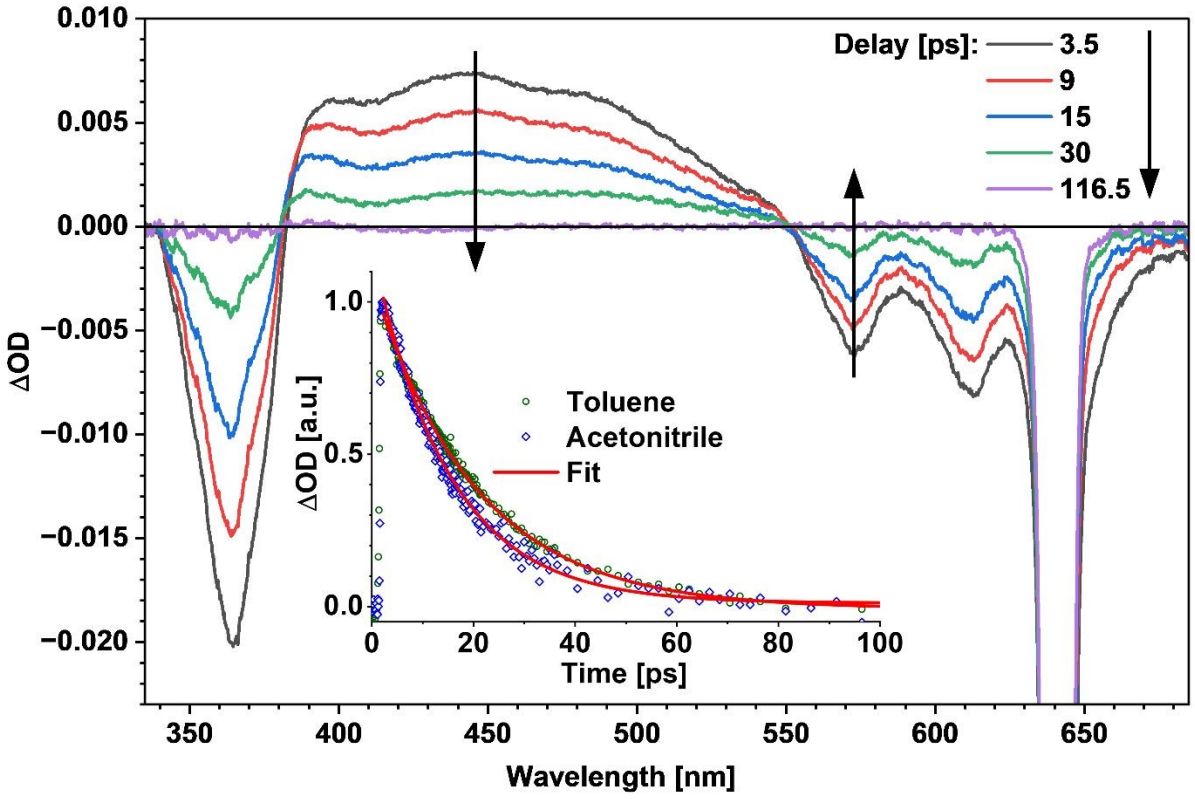

Figure 3. Transient absorption spectra of **3** in 10^{-5} M acetonitrile solution at 293 K, obtained at five different pump-probe delays: 3.5, 9, 15, 30, and 116.5 ps. Insert, fitting of the kinetics probed at 445 nm in acetonitrile (blue circles) and toluene (green circles) with a monoexponential decay function. The excitation wavelength was 642 nm.

View Article Online
DOI: 10.1039/D6CP01735E

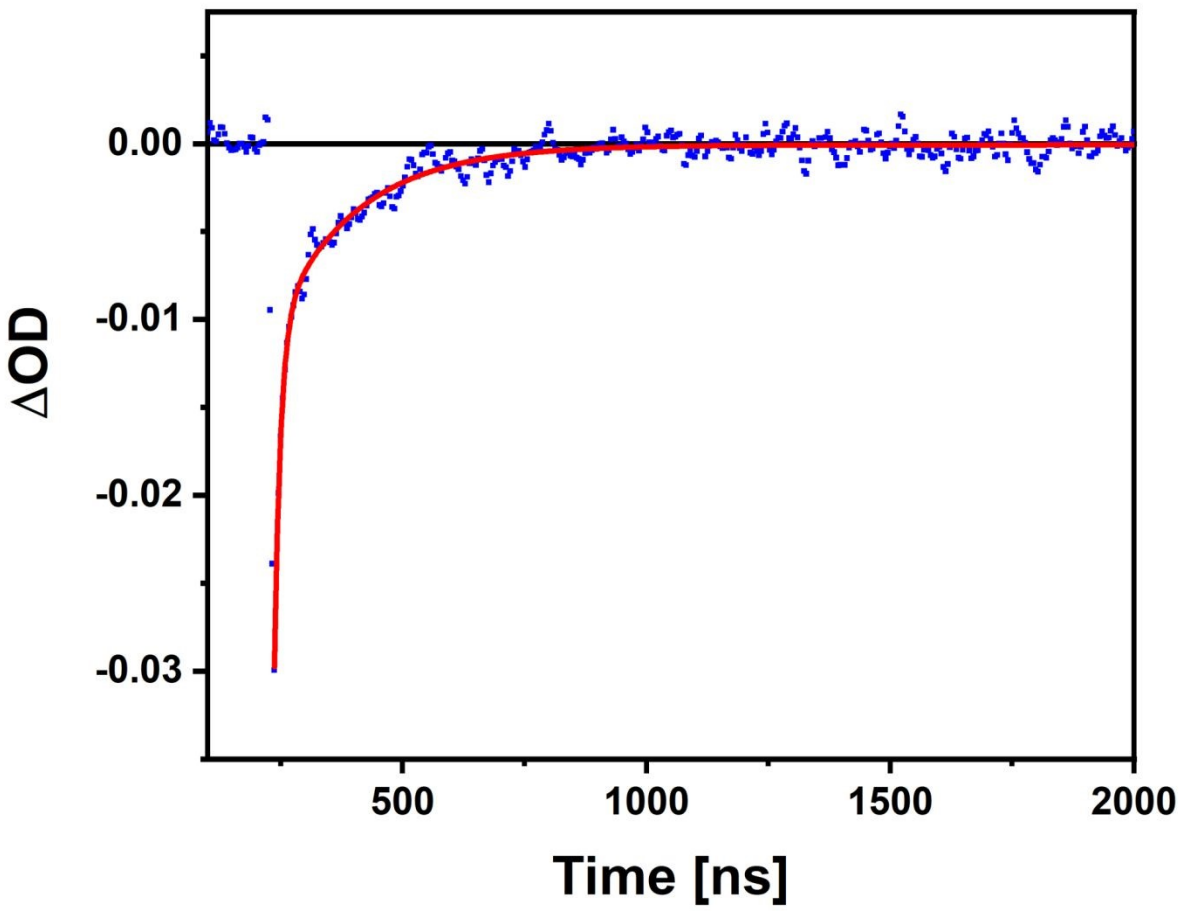

Figure 4. Kinetic profile of ground state repopulation, measured in 10^{-5} M acetonitrile solution at 293 K. The sample was excited at 363 nm and probed at 570 nm. The decay could be fitted with a biexponential function (red line).

View Article Online
DOI: 10.1039/D6CP01735E

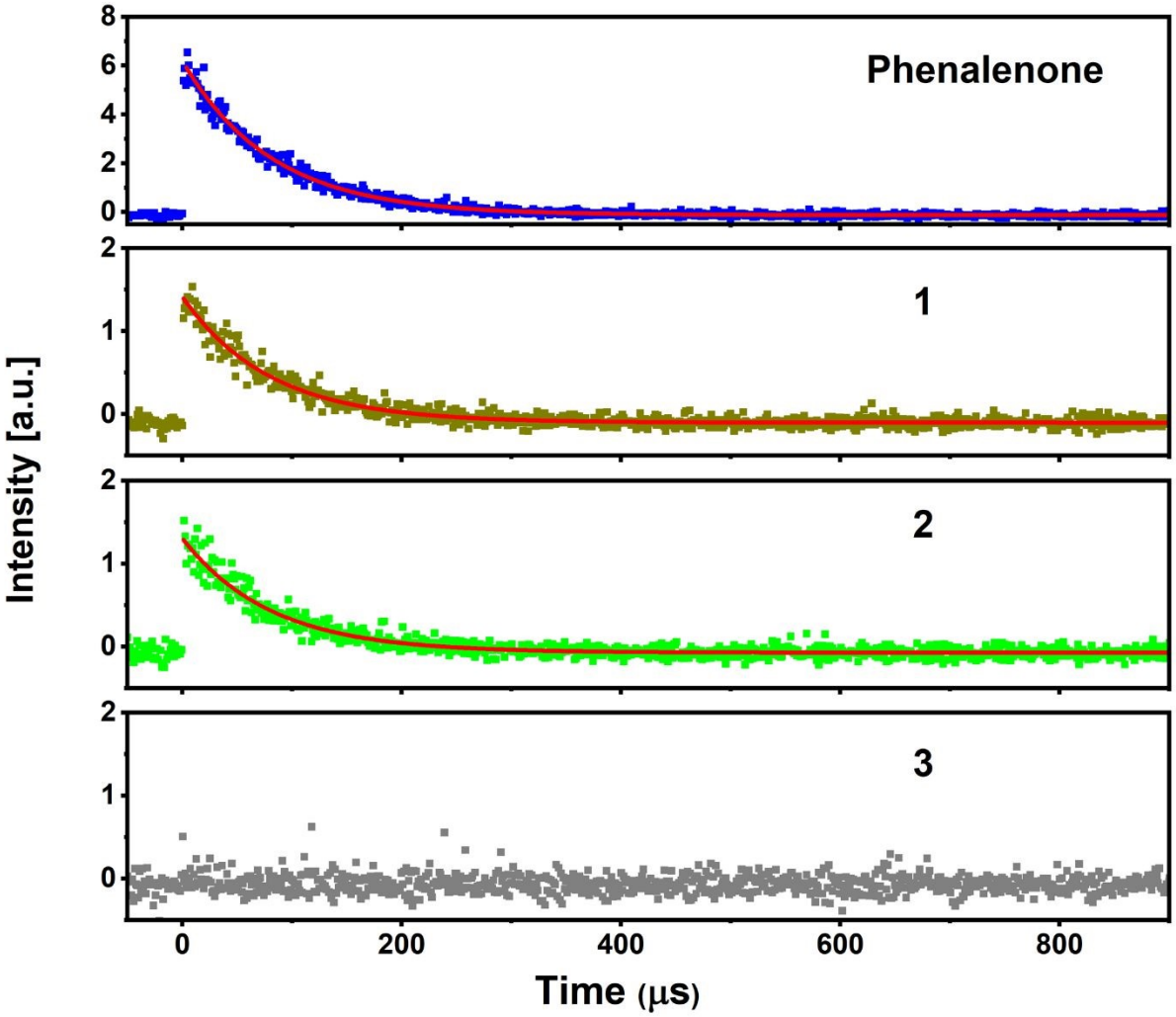

Figure 5. Kinetics of singlet oxygen phosphorescence decay. From top to bottom: 10^{-5} M acetonitrile solutions of phenalenone, **1**, **2**, and **3**. Excitation wavelength: 363 nm.

View Article Online
DOI: 10.1039/D6CP01735E

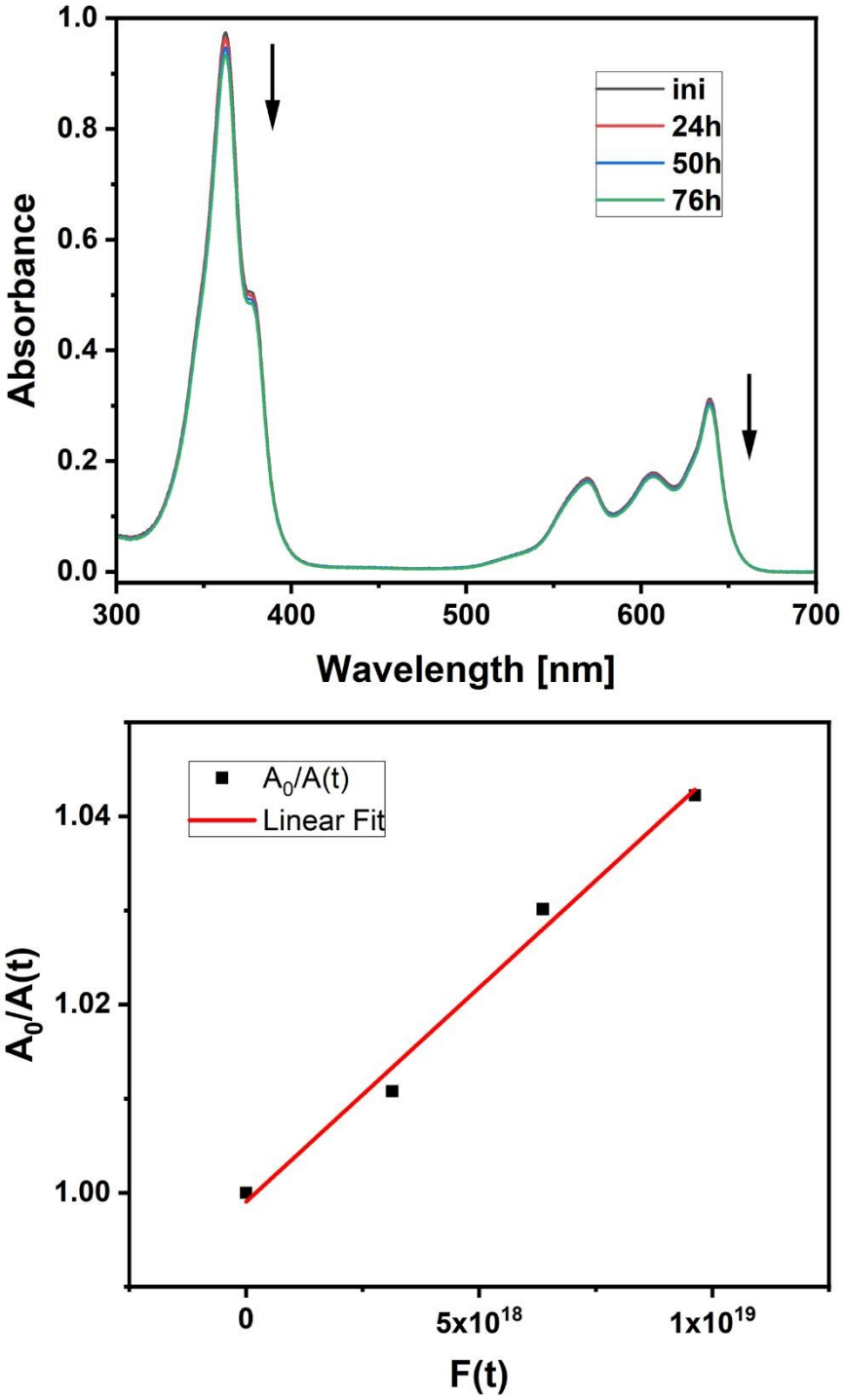

Figure 6. Top changes in the absorption spectrum of **2** in toluene irradiated for 24, 50, and 76 h with 369 nm LED (power of 92 mW). The photodegradation quantum yield was obtained from the slope of the plot of $A_0/A(t)$ vs F(t) (bottom). F(t) = N*total*(t)/A(t), A_0 and A(t) denote the absorbance values before and after irradiation at time t, and N*total*(t) is the total number of photons absorbed over t. The monitoring wavelength was 362 nm.

View Article Online
DOI: 10.1039/D6CP01735E

REFERENCES

1. J. C. Stockert, M. Cañete, A. Juarranz, A. Villanueva, R. W. Horobin, J. Borrell, J. Teixidó and S. Nonell, *Curr. Med. Chem.*, 2007, **14**, 997-1026.
2. I. Nieves, C. Hally, C. Viappiani, M. Agut and S. Nonell, *Bioorg. Chem.*, 2020, **97**, 103661.
3. Y. Yamada, Y. Miwa, Y. Toyoda, Q. M. Phung, K.-i. Oyama and K. Tanaka, *Catalysis Science & Technology*, 2023, **13**, 1725-1734.
4. S. Kato, M. Abe, H. Gröger and T. Hayashi, *ACS Catalysis*, 2024, **14**, 13081-13087.
5. S. E. Braslavsky, M. Müller, D. O. Mártire, S. Pörting, S. G. Bertolotti, S. Chakravorti, G. Koç-Weier, B. Knipp and K. Schaffner, *J. Photochem. Photobiol. B*, 1997, **40**, 191-198.
6. J. Waluk, *Chem Rev*, 2017, **117**, 2447-2480.
7. M. Kijak, K. Nawara, A. Listkowski, N. Masiera, J. Buczyńska, N. Urbańska, G. Orzanowska, M. Pietraszkiewicz and J. Waluk, *J. Phys. Chem. A*, 2020, **124**, 4594-4604.
8. P. G. Seybold and M. Gouterman, *J. Mol. Spectrosc.*, 1969, **31**, 1-13.
9. A. K. Mandal, M. Taniguchi, J. R. Diers, D. M. Niedzwiedzki, C. Kirmaier, J. S. Lindsey, D. F. Bocian and D. Holten, *J. Phys. Chem. A*, 2016, **120**, 9719-9731.
10. M. Gil, J. Dobkowski, G. Wiosna-Sałyga, N. Urbańska, P. Fita, C. Radzewicz, M. Pietraszkiewicz, P. Borowicz, D. Marks, M. Glasbeek and J. Waluk, *J. Am. Chem. Soc.*, 2010, **132**, 13472-13485.
11. T. Ono, D. Koga, K. Yoza and Y. Hisaeda, *Chem. Commun.*, 2017, **53**, 12258-12261.
12. D. Koga, T. Ono, H. Shinjo and Y. Hisaeda, *J. Phys. Chem. Lett.*, 2021, **12**, 10429-10436.
13. A. Listkowski, N. Masiera, M. Kijak, R. Luboradzki, B. Leśniewska and J. Waluk, *Chem. Eur. J.*, 2021, **27**, 6324-6333.
14. P. Ciąćka, P. Fita, A. Listkowski, M. Kijak, S. Nonell, D. Kuzuhara, H. Yamada, C. Radzewicz and J. Waluk, *J. Phys. Chem. B*, 2015, **119**, 2292-2301.
15. J. Michl, *Tetrahedron*, 1984, **40**, 3845-3934.
16. G. Rltzoulis, N. Papadopoulos and D. Jannakoudakls, *J. Chem. Eng. Data*, 1986, **31**, 146-148.
17. J. Ostapko, A. Gorski, J. Buczyńska, B. Golec, K. Nawara, A. Kharchenko, A. Listkowski, M. Ceborska, M. Pietrzak and J. Waluk, *Chem. Eur. J.*, 2020, **26**, 16666 – 16675.
18. J. D. Spikes, *Photochem. Photobiol.*, 1992, **55**, 797-808.
19. J. A. S. Cavaleiro, H. Gorner, P. S. S. Lacerda, J. G. MacDonald, G. Mark, M. G. P. M. S. Neves, R. S. Nohr, H. P. Schuchmann, C. van Sonntag and A. C. Tome, *Journal of Photochemistry and Photobiology a-Chemistry*, 2001, **144**, 131-140.
20. M. Paez-Perez and M. K. Kuimova, *Angew. Chem. Int. Ed.*, 2024, **63**, e202311233.
21. S.-C. Lee, J. Heo, H. C. Woo, J.-A. Lee, Y. H. Seo, C.-L. Lee, S. Kim and O.-P. Kwon, *Chem. Eur. J.*, 2018, **24**, 13706-13718.
22. A. Jamrozik, A. Gorski, B. Golec and J. Waluk, *J .Phys. Chem. C*, 2025, **129**, 22435-22442.
23. D. Sánchez-Garcia and J. L. Sessler, *Chem. Soc. Rev.*, 2008, **37**, 215-232.
24. W. Brenner, J. Malig, C. Oelsner, D. M. Guldi and N. Jux, *J. Porphyrins Phthalocyanines*, 2012, **16**, 651-662.

View Article Online
DOI: 10.1039/D6CP01735E

DATA AVAILABILITY

The data that support the findings of this study are available from the corresponding author upon reasonable request.